5th Joint International Symposium on Deformation Monitoring (JISDM), 20-22 June 2022, Valencia, Spain
DOI: http://doi.org/10.4995/JISDM2022.2022.13917

Assessment of accuracy and performance of terrestrial laser scanner in monitoring of retaining walls

Ali Algadhi[1, 2], Panos Psimoulis[1, 3], Athina Grizi[3], Luis Neves[3]

[1] Nottingham Geospatial Institute, University of Nottingham, Nottingham, UK, (aalgadhi@ksu.edu.sa)
[2] Department of Civil Engineering, King Saud University, Riyadh, KSA
[3] Department of Civil Engineering, University of Nottingham, Nottingham, UK,
(Panagiotis.Psimoulis@nottingham.ac.uk; A.Grizi@nottingham.ac.uk; Luis.Neves@nottingham.ac.uk)

Key words: *terrestrial laser scanner; deformation monitoring; retaining walls; accuracy; C2C; C2M; M3C2*

ABSTRACT

Retaining walls are a critical infrastructure of transportation networks and the monitoring of their condition is crucial for the efficient and reliable maintenance of the network. The condition of retaining walls is frequently assessed using qualitative criteria and visual inspection, which are susceptible to human-bias and errors. To improve the management of these structures, reducing the probability of failure and the maintenance costs, it is critical to develop more efficient, reliable and quantitative monitoring approaches for these structures. The current study aims to evaluate the performance of Terrestrial Laser Scanner (TLS) in deformation monitoring of retaining walls, based on the analysis of single scans (without registering the point clouds to build 3D models). The evaluation was based on a controlled experiment, where a wooden frame (1.5m x 1m) was used to simulate deformation scenarios for retaining walls, with an amplitude between 2 to 16 mm. A Leica RTC360 scanner was used to scan the wooden frame from distances varying between 10 to 27 m and angles varying between 0° to 20°. Five methods were applied to analyse the laser-scanner data and estimate the displacement: a target-based approach and four cloud-based approaches including the Cloud-to-Cloud (C2C), the Cloud-to-Mesh (C2M), the Multiscale-Model-to-Model-Cloud-Comparison (M3C2), and an alternative cloud-based method where the mean average of the point-cloud was used to estimate the displacement in the axis of the deformation. A Robotic Total Station Leica TS30 was also used to measure the deformation of the wooden frame and provide the ground truth values of the introduced deformation for each scenario. The results showed that the RTC360 had an accuracy of 1.3 mm with a confidence level of 95%.

I. INTRODUCTION

The potential of using the Terrestrial Laser Scanning technology (TLS) in the field of structural health monitoring has been the focus of many researchers (Kim *et al.*, 2019; Athanasopoulos-Zekkos *et al.*, 2020), due to the precise and practical solution that the TLS can provide compared to other instruments, such as inclinometers, strain gages and photogrammetry (Athanasopoulos-Zekkos *et al.*, 2020). In monitoring retaining structures, geometric deformations are the main defects that need to be monitored (Kim *et al.*, 2019; Athanasopoulos-Zekkos *et al.*, 2020). The TLS can also be used for monitoring non-geometric related defects in retaining walls, such as monitoring the change in temperature of concrete surface (Mukupa, 2017), cracks and long-term deterioration (Law *et al.*, 2018), moisture content (Suchocki and Katzer, 2018; Živec *et al.*, 2019) and dynamic deformation of structures (Jatmiko and Psimoulis, 2017).

The accuracy of monitoring the geometric deformations in retaining walls using the TLS has been investigated. Although some studies concluded that TLS could assess the performance of retaining walls in service (Oskouie *et al.*, 2016; Aldosari *et al.*, 2020; Al-Rawabdeh *et al.*, 2020; Jia *et al.*, 2021), in the study of Seo *et al.* (2019) it is suggested that the TLS cannot provide the level of accuracy that is required to monitor retaining walls within the construction phase, reaching the maximum daily deformation of 4 mm in their case.

The sources of errors in monitoring structures using the TLS can be categorised in three main types: (i) instrumental-related; (ii) errors related to the monitored surface; and (iii) cloud registration errors (Lague *et al.*, 2013). Furthermore, the method that is used to analyse the point clouds does also affect the accuracy of the monitoring results (Lague *et al.*, 2013; Seo *et al.*, 2019). Although the accuracy of this methods was investigated, further work is necessary to better understand and quantify the accuracy of laser-scanning in monitoring retaining walls and how the accuracy is affected by monitoring parameters, such as the scanning distance. In the current study, we evaluate the impact of the scanning distance and the angle of incidence in the accuracy of the deformation estimation.

The main principle of this study is that the estimation of the deformation derives from the comparative analysis between two single scans of two different states of the retaining wall. Apart from the impact of the scanning distance and the angle of incidence, the

performance of different methods of point-cloud analysis are examined for the estimation of the retaining wall deformation. Although, three different types of deformation of retaining wall were examined (lateral displacement, vertical displacement and tilt), only the results of the lateral displacement experiment are presented in this paper.

II. Experimental setup

A wooden frame (1.5 m x 1 m) was built to simulate the surface of a retaining wall which would be subjected to different types of deformation (see Figure 1). The horizontal displacement was introduced via a bolt on the back of the wooden frame and the movement was measured using a metallic measure tape attached to the frame arm (see Figure 1c). Five black/white paper targets were glued to five key locations on the wooden frame (the four corners and the centre) and used as reference points to monitor the change in the frame position (see Figure 1a).

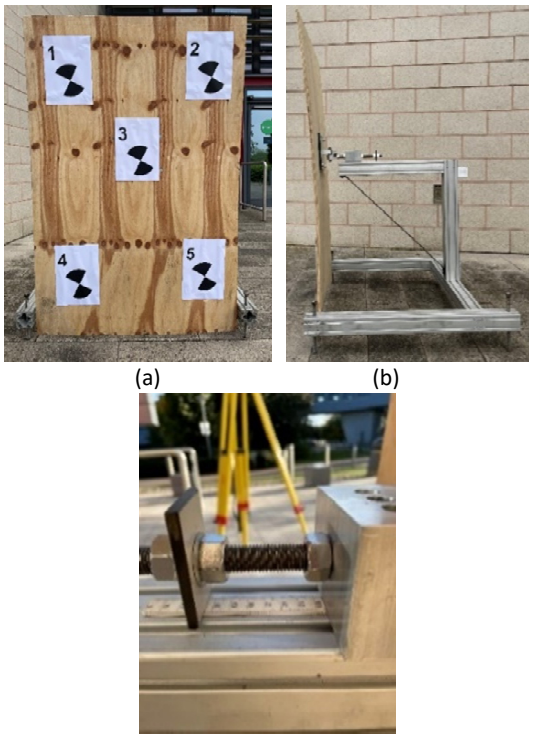

Figure 1. The designed wooden frame: (a) front view; (b) side view; and (c) bolt to adjust the frame position laterally.

A Leica RTC360 laser scanner was used to scan the wooden frame from six different scanning stations: three different scanning distances and two different incidence angles (see Figure 2). The scans were taken from 10 m, 20 m and 27 m scanning distances and with angles of incidence of 0° and 20° (see Table 1). A robotic total station (Leica TS30) was also used to provide the ground truth for the monitoring measurements. The application of RTS measurements in structural monitoring has been successfully assessed in experiments and real structural monitoring applications, proving to be reliable even for mm-level deformation (Psimoulis and Stiros, 2007; 2008). The TS30 was used in a singular location unlike the RTC360 that was used in six scanning stations. Three Leica GZT21 scanning targets were established on three wooden tripods on different locations in the field as shown in Figure 2. The main purpose for these targets was to introduce a common coordinate system for the point clouds. The TS30 was used to survey these targets before and after the experiment to ensure that the entire network (*i.e.* TS30 and the static targets) remained stationary during the experiment. The TS30 was also used to survey the targets that were glued to the wooden frame (see Figure 1a) to perform the monitoring process. The experiment was conducted outdoor, and the measurements were taken under the same weather condition as the experiment was completed on the same day.

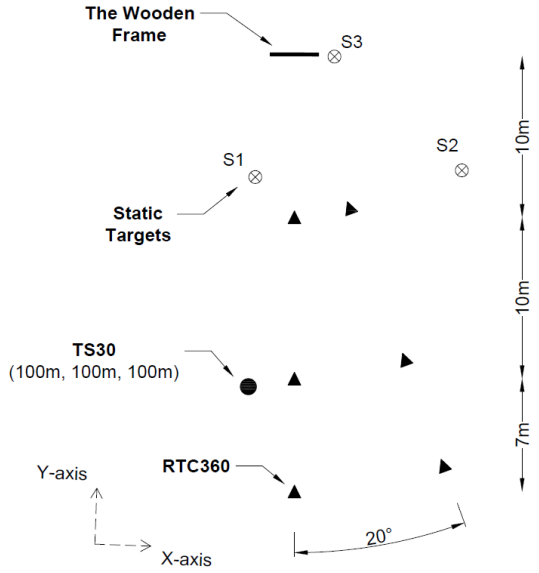

Figure 2. Figure Overview of the experimental site (top view), with the location of (i) RTC360, (ii) TS30, (iii) the wooden frame and (iv) the static targets. The Y-axis was parallel to the line between the TS30 and the static target "S1". This was the coordinate system that was introduced in the field using the TS30. This coordinate system was then rotated as explained in the data registration section. The drawing is not to scale.

Table 1. Experiment set-up and the scenarios of deformations that were simulated

	Experiment set-up		Deformation Scenario
	Distance [m]	Angle of incidence [degrees]	Lateral Disp. [mm] Initial
RTC360	10	0	2
	20	20	4
	27		8
TS30	20	0	16

The frame was firstly set up on one of the five states (*i.e.* deformation scenario) presented in Table 1. Then, the glued targets were surveyed using the TS30, by taking measurements in face left and face right. The

RTC360 was set to scan with the highest available resolution (*i.e.* 3 mm at 10 m) and by using the "double scan" function in order to remove any moveable objects captured during the scans. Each deformation scenario was examined for the three scanning distances and the two angles of incidence. After the completion of one of the deformation scenarios (taking measurements using the TS30 and scanning the frame using the RTC360 from six scanning stations), the wooden frame was set up on the next deformation scenario and the same procedure was applied.

III. Data registration

In any monitoring project, the measurements need to be registered in the same coordinate system. This step is not only essential to perform the monitoring (compare different states of the wooden frame) but also to compare the results that were taken by the RTC360 with those taken by the TS30. This section explains the process of introducing a common coordinate system for all the measurements (TS30 and RTC360). For the RTC360 point-clouds, each single scan was registered individually to that common coordinate system in order to perform the monitoring but not for the sake of building a 3D model of the scanned surface.

A Cartesian coordinate system was established based on the TS30 measurements; by defining the position of TS30 (X_o = 100 m, Y_o = 100 m and Z_o = 100 m) and setting the Y-axis where the TS30 was pointing towards the target "S1" (see Figure 2). Then, a line was fitted in the horizontal plane defined by X- and Y-axes, based on the targets that were glued to the wooden frame, as shown in Figure 3a. The fitted line was used to rotate the X-Y plane to make the X-axis parallel to the frame surface and Y-axis aiming perpendicular towards the frame surface (see Figure 3b). The Z-axis remained vertical pointing upwards. The lateral displacement was then calculated in the Y-axis.

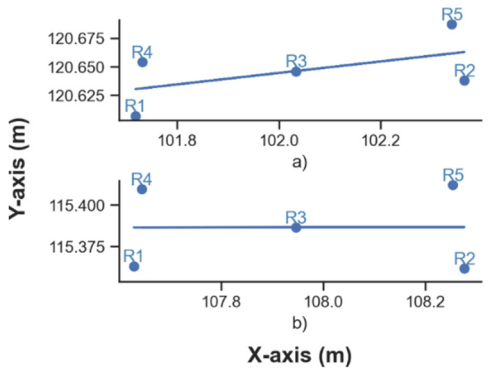

Figure 3. The five targets that were glued to the wooden frame along with the fitted line (top view): a) before, and b) after rotating the coordinate system in the X-Y plane.

The registration process for the RTC360 scans was executed using the seven-parameter-transformation (Helmert transformation) method (Zavoti and Kalmar, 2016). The seven parameters are: three translations between the two coordinate systems (t_x, t_y, t_z), three rotation parameters (around X, Y and Z axes – ω, φ, κ), and one scale factor λ. The three static targets (see Figure 2) were used to provide nine equations (three equations for the coordinates of each target). Two additional equations allowed the Least Square's method to be adjusted to find the statistical solution.

IV. Principles of the monitoring methods

Two approaches were adopted to estimate the deformation of the wooden frame using the RTC360 point-clouds: (i) target-based; (ii) cloud-based. In the target-based approach, the coordinates of the five targets were used to estimate the deformation of the wooden frame (see Figure 1a). The coordinates of the targets were extracted via an automated feature to identify the centre of the targets using the Leica Cyclone software (Leica Geosystems, 2021). The coordinates of the five targets were calculated for the initial-reference position of the wooden frame without any induced lateral displacement and for each of the scenarios of lateral displacement, as the average of the coordinates of the five points. The lateral displacement was then calculated based on the difference between each scenario and the reference position of the wooden frame. The same approach was adopted to calculate the lateral displacement based on the TS30 measurements, which was used as the true amplitude of lateral displacement.

In the Cloud-based approach, the change was calculated in two sets of clouds; the first is called the reference cloud and the other called the compared cloud. There are three well-known techniques to calculate the distance between the point-clouds: Cloud-to-Cloud (C2C), Cloud-to-Mesh (C2M), and Multiscale-Model-to-Model-Cloud-Comparison (M3C2). These methods were performed using an open-source software; CloudCompare (2021). The C2C method finds for each point in the compared cloud its closest point in the reference cloud. This method was improved by fitting a surface over a group of neighbouring points in the reference cloud with using the K-nearest neighbours' algorithm (K=6 in this experiment). The surface was fitted using the Least Square's method. The resulted distances were split in X, Y and Z components and only the component in the Y-axis was used to compute the lateral displacement. The C2M method was executed by creating a surface mesh for the point clouds in "initial" state scans (from six scanning positions). The fitted surface for the reference cloud was "2.5D quadric" and the closest distance for each point in the compared cloud was then calculated. The M3C2 method was performed using the entire reference cloud as core points, a normal scale (diameter) and a projection scale (diameter) of 0.018 m, and with a maximum depth (maximum distance to be calculated) of 0.090 m. The calculation mode was set to be in "Horizontal" and the preferred

orientation was set to be along the "-Y" axis. Additional information on these three methods (C2C, C2M & M3C2) can be found in Lague *et al.* (2013). Since these methods calculate the distance between the two point-clouds for large number of points in the point-clouds, the statistical mode of the calculated distances was used as the magnitude of lateral displacement. An additional Cloud-based method for estimating the lateral displacement in the wooden frame was proposed through monitoring the mean of each cloud in the Y-axis. These four cloud-based methods as well as the target-based method was analysed and compared to the ground truth measurements which were taken from the Leica TS30.

V. MONITORING RESULTS

The first step of the analysis was to check whether the static targets, which were used to define the coordinate system remain stable during the measurements. Table 2 presents the difference in coordinates of the static targets that were surveyed before and after conducting the experiment using the TS30. The change in coordinates did not exceed 1 mm for any of the targets and they were distributed in different axes, meaning that the targets were stable during the experiments and susceptible only to random errors.

Table 2. The change in coordinates of the static targets before and after the experiment using the TS30

Target ID	Ex [mm]	Ey [mm]	Ez [mm]
S1	-1	0	1
S2	0	0	0
S3	-1	0	0

For the RTC360, the clouds were registered to the local coordinate system that was defined by the TS30 measurements. Initially, each point-cloud of the RTC360 was in an arbitrary coordinate system, which was transformed by using the three static targets, which were also surveyed by the TS30, as reference points. The standard deviations of the seven transformations parameters (t_x, t_y, t_z, ω, φ, κ, λ), which derived as the diagonal elements of the variance-covariance matrix, are plotted in Figure 4. The accuracy of the coordinate transformation of the point clouds was evaluated by plotting the errors in defining the coordinates of the static targets (see Figure 5). The value of zero corresponds to the true-reference value, as it was derived from the TS30 measurements. These errors show the accuracy of the RTC360 point-clouds as well as the accuracy of the least square solution (since the Least Square's method estimates the optimum but not the exact solution). In addition, the errors were influenced by the automatic feature tool to define the centre of the targets in the Leica Cyclone software (Leica Geosystems, 2021). It is noticeable that the error is distributed in the three static targets, as it is expected from the Least Squares adjustments solution. The errors mostly fall in the zone of 0.5 mm. However, this was not the case for some scans, such as the scan of "initial" state that was taken from 20m and angle of incidence of 0°. Theoretically, the error of defining the static targets is not affected by the deformation scenario as the static targets remained stationary. This was observed in Figure 5 where the errors seem to be constant regardless of the deformation scenario.

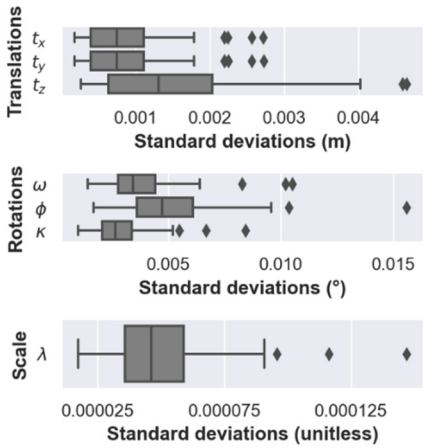

Figure 4. Box plots for the standard deviations for the transformation parameters to register the RTC360 clouds in the local coordinate system (introduced using the TS30 measurements). The middle line of the box corresponds to the statistical median whereas the box expresses the 25 and 75% thresholds of the distribution. The box is also referred to as the Interquartile range (IQR). The two bars express the minimum and maximum values which have a distance of 1.5*IQR from the first and third quartiles. The external points show the outliers.

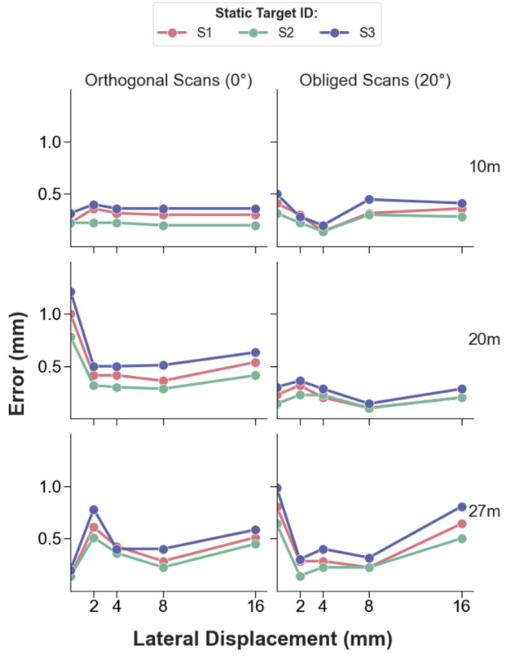

Figure 5. Error of the 3D-coordinate of the three static targets from the RTC360 scans, after the coordinate system transformation. The errors are grouped by the scanning distance and angle of incidence. The error is with respect the coordinates estimation using the TS30 measurements. The error of zero magnitude of lateral displacement referrers to the "initial" state of deformation.

After registering all the point-clouds, the monitoring of the lateral displacement in the wooden frame was performed. The "initial" state of the wooden frame, as shown in Table 1, was used as the reference state, against which the four other scenarios were compared. The deformations were estimated using the five monitoring methods: (i) target method, (ii) cloud-mean method, (iii) C2C method, (iv) C2M method, and (v) M3C2 method. After obtaining the lateral displacements, the results were compared to the TS30. Figure 6 shows the absolute errors in the estimated lateral displacement for each monitoring method. The results are plotted according to the scanning distance and the angle of incidence. In general, it is observed that the target-method and the cloud-mean method obtained results of similar accuracy and very close to the measurements that were taken by the TS30. Obtaining very similar values and pattern means that these two methods are validated, and are expected to obtain consistence deformation estimation. Regarding the other three cloud comparison techniques (C2C, C2M and M3C2), they resulted in errors of less than 2.5mm and they seemed to be generally less accurate than the target and cloud-mean methods.

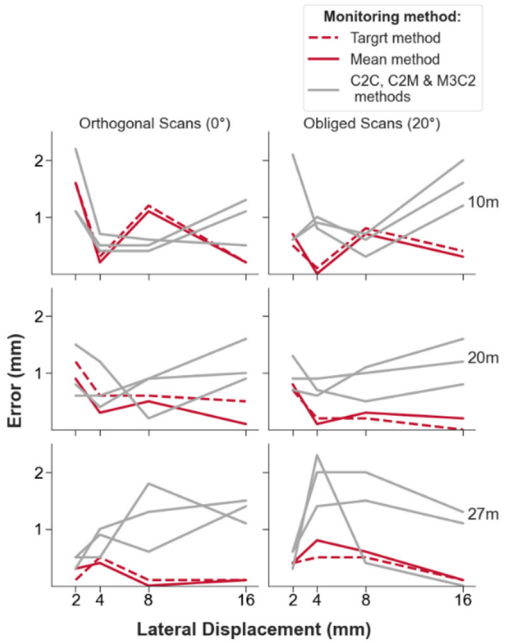

Figure 6. The absolute errors in estimating the lateral displacements for the wooden frame (the zero magnitude of error refers to the TS30 estimation).

The target and cloud-mean methods obtained similar results and pattern over different angles of incidence.

Characteristic example is the scenarios of scanning distance 10m, where for both incidence angles the error pattern was similar (see Figure 6). Furthermore, the similarity of the error pattern is mainly observed between the two angles of incidence, which means that the error seems to be affected by the scanning distance more than the angle of incidence (for angles of the examined range: from 0° to 20°).

Since all the comparisons were made between independent scans, the common pattern of the errors should be the result of a common error between the scans. One potential error could be caused by the coordinate transformation, which however was characterised by error about 0.5mm, as it was indicated in Figure 5. Furthermore, potential errors of TS30 should not have significant impact on the scans through the coordinate system definition, as the TS30 error was limited in less than 1 mm, reflected on static targets coordinates definition. Also, the TS30 measurements, which were made in face-left and face-right had an average misalignment of less than 1 mm, indicating that potential error of TS30 should not affect the displacement estimations in Figure 6. Another parameter which seems to affect the performance of the point-clouds accuracy is the network geometry of the static targets and their relative position with respect to the TLS position. The geometry of the static targets affects the accuracy of the point-clouds as was investigated by Fan *et al.* (2015). This is supported by the fact that as the scanning distance in Figure 6 decreases, the error patterns of the target and cloud-mean methods for the two incidence angles become closer. That is because the effect of the scanning angle in the geometry of the static targets increases as the distance increases.

To further investigate the accuracy of each monitoring method, the average error of each method was plotted in Figure 7. This average error was calculated based on all the errors from the six different scanning stations (with different scanning distances and incidence angles). The standard deviation of that average error was multiplied by two and was also plotted in Figure 7 to show the 95% confidence level of that error. Hence, the total length of the bar represents the expected error of each monitoring method with a confidence level of 95%. The deformations that were estimated using the cloud-mean method as well as the target method provided the highest accuracies among the other methods. Generally, the accuracy of all the methods were about 2 mm with 95% confidence level. The average of the errors for the mean and target methods were 0.45 mm and 0.48 mm with standard deviations of 0.39 mm and 0.40 mm, respectively. Although the M3C2 had an average error similar to the values estimated by the C2C and C2M, the standard deviation of the errors was the overall lowest (0.37 mm). Therefore, the M3C2 had an overall accuracy of 1.7 mm with 95% confidence level, which is better than those obtained by the C2C and C2M methods (see Figure 7). The C2M method provided the least accurate estimation, and that mainly because it calculates the Euclidean distance to the mesh (*i.e.* does not calculate the distance along the desired axis, Y-axis, whereas the C2C and M3C2 methods do).

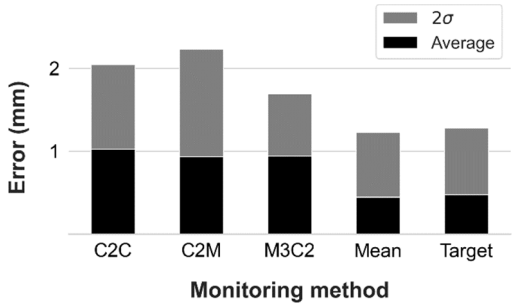

Figure 7. Bar plot for the average errors for each monitoring method. The black part of the bar represents the average error whereas the full length of the bar shows the error budget with a confidence level of 95%. The zero magnitude of error refers to the TS30 estimation.

The effect of the scanning distance and angle of incidence was also studied. Figure 8 shows the average errors of each monitoring method for the various examined scanning distance, whereas the errors were grouped by the angle of incidence in Figure 9. It is expected that the error increases as the scanning distance and angle of incidence increase; however, this was not always the case for the mean and target methods. For example, errors in the orthogonal scans in Figure 8 were decreasing as the scanning distance increases. Since this was not consistent among all the results, for example the error at a scanning distance of 27 m in Figure 9 was smaller in the orthogonal scans (for the cloud-mean and target methods) than the obliged scan. Consequently, these errors were mainly affected by the registration accuracy.

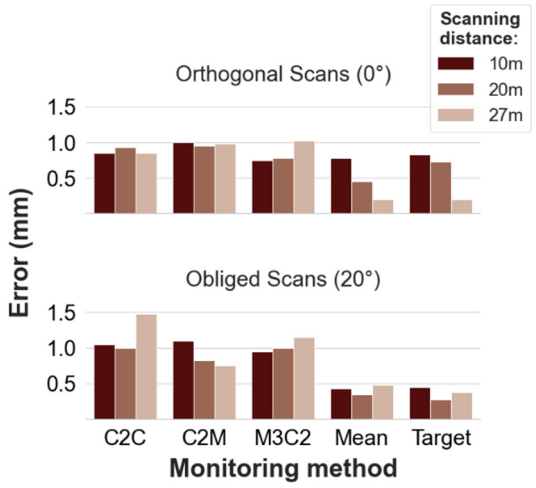

Figure 8. Bar plot for the average errors for each monitoring method filtered by the scanning distance (the zero magnitude of error refers to the TS30 estimation).

Similarly, the average errors were plotted for each monitoring method filtered by the deformation scenario in Figure 10. The C2C and M3C2 methods, which use the raw point clouds to estimate the displacement, seemed to have better accuracies when the introduced displacement was small. The mean and target methods did not have a clear pattern and the errors seemed to be just random errors. It is important to mention that since the deformation results for the mean and targets were almost identical over all the presented figures, these methods are most efficient methods for estimating the lateral displacement in the wooden frame.

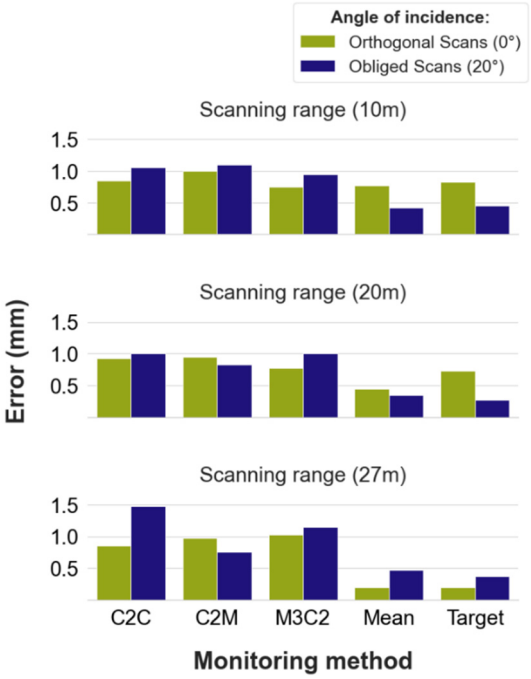

Figure 9. Bar plot for the average errors for each monitoring method filtered by the angle of incidence (the zero magnitude of error refers to the TS30 estimation).

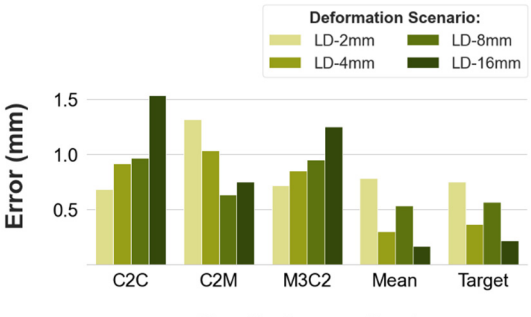

Figure 10. Bar plot for the average errors for each monitoring method filtered by the deformation scenario (the zero magnitude of error refers to the TS30 estimation).

VI. Conclusion

This paper investigated the effect of the scanning distance and angle of incidence on the accuracy of monitoring lateral displacements in a wooden frame that was designed to simulate the deformations of retaining walls. Various methods were used for estimating the deformation of the wooden frame using single scans (without building a 3D model of the scanned surface). The results showed that the cloud-mean method obtained the best accuracies, and its performance was very similar to the target method. The results showed also that the cloud comparison techniques (C2C, C2M and M3C2) are capable of estimating the lateral displacement in the wooden frame using the statistical mode of the calculated

distances of the two point-clouds. The results showed also that the accuracy was more affected by the accuracy of the coordinate transformation and the geometry of the static targets. The research findings suggest that the scanning distance and the angle of incidence are not the main sources of error.

The findings of this study have to be seen in light of some limitations. In this study, the reference coordinate system was introduced by using the TS30 measurements whereas if the RTC360 was used in practice, the first scan would be used as the reference coordinate system. This, however, might introduce a large error in the registration process, which was eliminated in this study. In addition, the use of only three static targets leaves no independent checks for the accuracy of the scans. The use of single scans in this study eliminated the error caused by registering point-clouds that are taken for a surface from different scanning positions to build the 3D model. Furthermore, the results showed the performance of the TLS for monitoring only the lateral displacements. Therefore, future research should address the performance of the TLS in monitoring other deformations scenarios for retaining walls. The effect of distance and angle of incidence can be investigated further. Since in practice, it is expected to scan retaining walls from a different location at a time, it is important to investigate the accuracy of the deformation estimations with different scanning set-up. For example, the scan of "initial" state that was taken orthogonally with a scanning distance of 10 m can be used as the reference cloud and be compared to the scan of "lateral displacement (2 mm)" state that was taken with an angle of 20° and a scanning distance of 20 m.

References

Aldosari, M., Al-Rawabdeh, A., Bullock, D., and Habib, A. (2020). A Mobile LiDAR for Monitoring Mechanically Stabilized Earth Walls with Textured Precast Concrete Panels. *Remote Sensing,* Vol 12, No.2, pp. 306.

Al-Rawabdeh, A., Aldosari, M., Bullock, D., and Habib, A. (2020). Mobile LiDAR for Scalable Monitoring of Mechanically Stabilized Earth Walls with Smooth Panels. *Applied Sciences*, Vol 10, No. 13, pp. 4480.

Athanasopoulos-Zekkos, A. A., Lynch, J., Athanasopoulos-Zekkos, D., Grizi, A., Admassu, K., Benhamida, B., Spino R. J., and Mikolajczyk, M., (2020). Asset Management for Retaining Walls. Michigan: University of Michigan.

CloudCompare (2021). CloudCompare v2.12 beta [Windows 64-bit]. Available from <http://www.cloudcompare.org/>

Fan, L., Smethurst, J.A., Atkinson, P.M., and Powrie, W. (2015). Error in Target-Based Georeferencing and Registration in Terrestrial Laser Scanning. *Computers & Geosciences,* Vol 83, pp. 54-64.

Jatmiko, J. and Psimoulis, P., (2017). Deformation Monitoring of a Steel Structure Using 3D Terrestrial Laser Scanner (TLS). In: *Proceedings of the 24th International Workshop on Intelligent Computing in Engineering*, Nottingham, UK. pp. 10-12.

Jia, D., Zhang, W., and Liu, Y. (2021). Systematic Approach for Tunnel Deformation Monitoring with Terrestrial Laser Scanning. *Remote Sensing,* Vol 13, No. 17, pp. 3519.

Kim, M.-K., Wang, Q., and Li, H. (2019). Non-Contact Sensing Based Geometric Quality Assessment of Buildings and Civil Structures: A Review. *Automation in Construction,* Vol 100, pp. 163-179.

Lague, D., Brodu, N., and Leroux, J. (2013). Accurate 3D Comparison of Complex Topography with Terrestrial Laser Scanner: Application to the Rangitikei Canyon (N-Z). *ISPRS Journal of Photogrammetry and Remote Sensing,* Vol 82, pp. 10-26.

Law, D.W., Silcock, D., and Holden, L. (2018). Terrestrial Laser Scanner Assessment of Deteriorating Concrete Structures. Structural Control and Health Monitoring, Vol 25, No. 5, e2156

Leica Geosystems, AG. (2021). Leica Cyclone v2021.1.1 [Windows 64-bit]. Available from <https://leica-geosystems.com/>

Mukupa, W. (2017). Change Detection and Deformation Monitoring of Concrete Structures Using Terrestrial Laser Scanning. Nottingham: University of Nottingham.

Oskouie, P., Becerik-Gerber, B., and Soibelman, L. (2016). Automated Measurement of Highway Retaining Wall Displacements Using Terrestrial Laser Scanners. *Automation in Construction*, Vol 65, pp. 86-101.

Psimoulis, P., and Stiros, S. (2007). Measurement of deflections and of oscillation frequencies of engineering structures using Robotic Theodolites (RTS). *Engineering Structures*, 29(12), pp. 3312-3324.

Psimoulis, P., and Stiros, S. (2008). Experimental assessment of the accuracy of GPS and RTS for the determination of the parameters of oscillation of major structures. *Computer-Aided Civil and Infrastructure Engineering*, 23(5), pp. 389-403.

Seo, H.J., Zhao, Y., and Wang, J. (2019). Monitoring of Retaining Structures on an Open Excavation Site with 3D Laser Scanning. In: International Conference on Smart Infrastructure and Construction 2019 (ICSIC) [online] Cambridge, UK. *ICE Publishing*, pp. 665-672.

Suchocki, C., and Katzer, J. (2018). Terrestrial laser scanning harnessed for moisture detection in building materials - Problems and limitations. *Automation in Construction,* Vol 94, pp. 127-134.

Závoti, J., and Kalmár, J. (2016). A Comparison of Different Solutions of the Bursa–Wolf Model and of the 3D, 7-Parameter Datum Transformation. *Acta Geodaetica et Geophysica,* Vol 51, No. 2, pp. 245-256

Živec, T., Anžur, A., and Verbovšek, T. (2019). Determination of rock type and moisture content in flysch using TLS intensity in the Elerji quarry (south-west Slovenia). *Bulletin of Engineering Geology and the* Environment, Vol 78, No. 3, pp. 1631-1643.